Analysis of switching properties of porous ferroelectric ceramics by means of first-order reversal curve diagrams

Laurentiu Stoleriu and Alexandru Stancu
Faculty of Physics, "Alexandru Ioan Cuza" University, Iasi, 700506, Romania

Liliana Mitoseriu
Faculty of Physics, "Alexandru Ioan Cuza" University, Iasi, 700506, Romania and DIChePP, University of Genoa, P.le Kennedy 1, Genoa I-16129, Italy

Daniele Piazza and Carmen Galassi
CNR-ISTEC, Via Granarolo 64, I-48018 Faenza, Italy

(Received 31 May 2006; revised manuscript received 21 September 2006; published 8 November 2006)

Particular aspects of the switching properties of the Nb-PZT ceramics with anisotropic porosity (40% relative porosity) were investigated by comparison with the dense ceramics (5% relative porosity) of the same composition by means of the first-order reversal curve (FORC) analysis. The reversible/irreversible components give different contributions to the total polarization: A sharp FORC distribution with an almost negligible reversible component is characteristic to the dense material, while a broad distribution with an important reversible component is characteristic for the porous one. The coercivity corresponding to the maximum of the irreversible component is the same irrespective to the sample density and pore's configuration with respect to the electrodes: $E_{c,M}=1.5$ kV/mm, while the bias fields are zero for the dense ceramic, small and positive; $E_{\mathrm{bias},M}=50$ V/mm, when the major axis of the elongated pores is parallel with the electrodes and negative; $E_{\mathrm{bias},M}=-100$ V/mm, when this axis is perpendicular to the electrodes. The influence of the dipolar coupling leading to such bias fields is explained by considering that the particular microstructure is causing a symmetry breaking, decoupling the dipolar interaction (forward or laterally). A dipolar (discrete) model with random orientations of the dipoles' directions was used to simulate this confinement effect. The calculated FORC diagrams lead to the same type of bias as the experimental ones, proving that the lateral confinement gives an intrinsic contribution to the biased $P(E)$ loops observed for the porous ceramics. In addition with other possible extrinsic contributions, this dipolar coupling can be a source of the built-in field in confined ferroelectric structures. The experimental FORC distribution was used as input in a Preisach-type model to recompose the major and symmetric minor hysteresis loops and a remarkable agreement with the experimental data was obtained. The FORC method proves to be an excellent tool in describing the ferroelectric systems, simulating polarization experiments, and predicting outputs of the circuits with ferroelectric capacitors. In the particular case of the porous anisotropic ceramics, the combined experimental and analytical FORC analysis allowed us to probe and to describe qualitatively the presence of the bias field as a result of the geometrical confinement.

DOI: 10.1103/PhysRevB.74.174107 PACS number(s): 77.84.Dy, 77.80.Dj, 77.80.Fm

I. INTRODUCTION

The Preisach formalism was largely applied for describing the switching properties of ferroics, particularly ferromagnetic,[1–3] superconductors,[4] spin glasses,[5] and, more recently, the polarization and piezoelectric responses in ferroelectric systems.[6–13] The same model is now used in the modeling of hysteretic phenomena in spin-transition materials (temperature, light-induced, and pressure hysteresis).[14,15]

When applied to ferroelectric switching, it is based on the assumption that the system is described by a collection of microscopic bistable units ("hysterons") having statistically distributed coercive and bias fields. Each dipolar unit is characterized by a rectangular hysteresis loop (Fig. 1) and its status is determined by the actual field and by the history of the applied external fields. In the original form of the theory, named classical Preisach model (CPM), the coercive and bias field distributions are considered statistically stable or, in other words, that these distributions are not dependent on the system state. Mayergoyz[16] has demonstrated that the necessary and sufficient conditions for a system to be correctly described by a CPM are the wiping-out (or deletion) and congruency properties. A hysteretic system will present the wiping-out property when it returns in the same ferroelectric state after performing a minor loop. The second property refers to the shape of the minor loops measured in the same field range; if all these minor loops are congruent within a given field range and this property does not depend on the actual field range used in the experiment, the system obeys the congruency property. A physical system correctly described by a CPM will be referred to as a classical Preisach system (CPS). In spite of the difficulty of fully demonstrating the validity of these requirements for a real ferroic sample, the CPM description is widely applied to numerous switchable systems.

The polarization of a CPS under any sequence of field is a sum of the overall hysterons' contributions weighted by their characteristic Preisach function, which is a 3D distribution of the switching units over their coercivity E_c and bias field E_{bias}: $\rho(E_c, E_{\mathrm{bias}})$.[3]

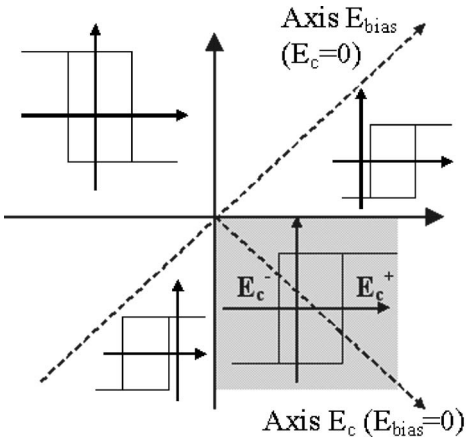

FIG. 1. The Preisach plane: a switching unit ("hysteron") is characterized by a rectangular hysteresis loop with the characteristic coercivities E_c^+, E_c^-; their distribution over (E_c^+, E_c^-) or, equivalently, over (E_c, E_{bias}) is the Preisach distribution.

One limitation in implementing the Preisach approach for ferroelectrics is coming from the difficulty in attributing a physical entity to the elementary switching unit. It was proposed that the hysteron can be either associated to an individual dipole or group of dipoles or to the ferroelectric domain walls moving under a stochastically defined pinning potential.[7,17] Therefore, even without a well-defined microscopic picture, it is still possible to replace the ferroelectric system by its formal representation as a unique distribution function of switching units with various coercivities and bias fields. These have as an origin the dipolar and stress fields that can be locally very different in a real ferroelectric sample, thus statistically distributed.

For an intuitive physical meaning of the local switching responses, we recall the piezoresponse force microscopy (PFM) results reported for various ferroelectric structures.[18–22] By this method, local vibrations of the sample surface through the tip and cantilever, induced by a testing ac signal applied between the conductive tip and the bottom electrode of the ferroelectric sample, are detected.[21] In the PFM experiments, hysteresis loops are obtained by sweeping the bias voltage and recording the piezoresponse signal while the tip is kept fixed above the desired nanoscale region of the sample. In this way, a field-induced local deformation under the tip produced by the converse piezoelectric effect of the ferroelectric is imaging the local domain structure and measuring local hysteresis loops. Local investigations in a given ferroelectric sample demonstrated a significant variability in local switching behavior caused by many reasons, such as local different cystallographic orientations and symmetry, local polar or charged defects, local variations of the composition, etc.[23–25] As a consequence, various types of loops, with distributed coercivities and bias fields (i.e., with different shifts along the field axis) are normally obtained. The macroscopic $P(E)$ loops result as a statistic sum (weighted convolution) of the local switching responses.[24] As a physical interpretation of the hysteron, the local $P(E)$ hysteresis loop as probed at nanoscale by the PFM experiments might be considered for a rough approximation. Although the distributed local loops over various coercivities and bias fields are supporting this idea, a few important observations have to be considered when proposing this interpretation. (i) The piezoelectric and polarization responses in the PFM are obtained under highly inhomogeneous electric fields as created by the small radius tip (point charge) which acts as top electrode. The switching process under inhomogeneous fields might involve completely different domain mechanisms and dynamics than the nucleation-growth as determined for the ferroelectric switching under homogeneous fields,[26] thus giving rise to different polarization-field responses. (ii) Even though the PFM responses are obtained at nanoscale, they are still far from being so "local" as needed by the model of "hysteron." Although the ferroelectric regions under the tip are mainly giving the polarization response (since the field is concentrated primarily in the surface region), some lateral and underneath domains still give small contributions, so that the measured PFM loops are already convoluted responses.[21] (iii) Due to the strong reduction of the field under the tip (depending on the sample and environment dielectric characteristics), the PFM response is mainly a surface one, while the overall ferroelectric volume contributes to the macroscopic $P(E)$ loops. In any case some features resulting from the PFM experiments are proving the high degree of the local variability of the switching parameters (in particular, the coercivity and bias fields), as postulated by the Preisach model.

Once we know the Preisach distribution, the ferroelectric polarization under any field sequence and history can be calculated. Further, it is possible to simulate the responses of any circuit containing ferroelectric capacitors by simulators [as, for example, simulation program with integrated circuit emphasis (SPICE)]. This information can bring essential contributions for designing and describing large scale and high speed integrated ferroelectric memory devices.

A different approach inspired by the Preisach modeling is based on the first-order reversal curves (FORC) distribution. The use of a system of FORCs to identify the Preisach distribution of a CPS was proposed by Mayergoyz.[4] Pike has extended the applicability of the method to any hysteretic system (CPS or not),[27] as a model independent experimental method. In this way, the method has a higher degree of generality, being not limited to any model restriction. It was extensively applied in past years for describing various phenomena in ferroics, such as switching in magnetic recording media, magnetic properties of spin glasses, ferrofluids and geological ferromagnetic systems,[27–29] thermal hysteresis in systems with spin transitions,[30] and polarization reversal characteristics of ferroelectrics.[12,31] It involves measurements of asymmetric minor hysteresis loops obtained by cycling the sample between saturation E_{sat} and a variable reversal field $E_r \in (-E_{sat}, E_{sat})$ according to the following sequence: (i) Saturation under a positive field $E \geqslant E_{sat}$; (ii) ramping the field down to the reversal value E_r, when the polarization follows the descending branch of the major hysteresis loop (MHL); (iii) increasing the field back to the positive saturation (during this process the polarization is a function of both the actual field E and of the reversal field E_r). The FORC family starting on the descending MHL branch is

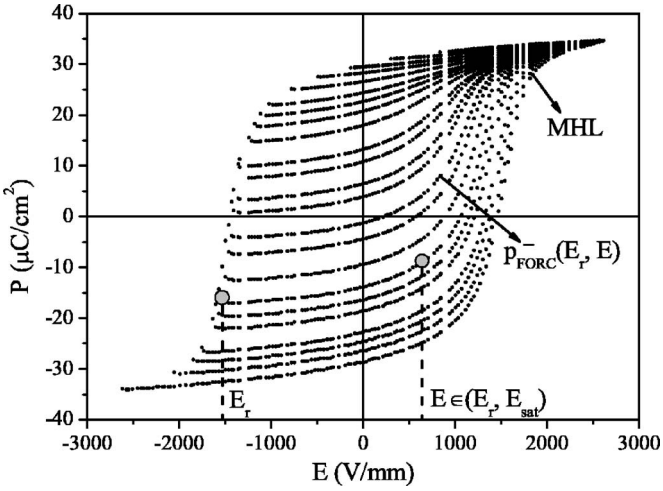

FIG. 2. The definition of the first order reversal curve (FORC) $p^-_{\mathrm{FORC}}(E_r,E)$ together with the experimental MHL and a few experimental FORCs recorded for the dense Nb-PZT ceramic.

denoted as $p^-_{\mathrm{FORC}}(E_r,E)$ (as represented in Fig. 2). In a similar way, the FORCs $p^+_{\mathrm{FORC}}(E_r,E)$ can be obtained using the ascending branch of the MHL. The FORC diagram is a contour plot of the FORC distribution which is defined as the mixed second derivative of polarization with respect to E and E_r:[27,28,32]

$$\rho^-(E_r,E) = \frac{1}{2}\frac{\partial^2 p^-_{\mathrm{FORC}}(E_r,E)}{\partial E_r \partial E} = \frac{1}{2}\frac{\partial \chi^-_{\mathrm{FORC}}(E_r,E)}{\partial E_r}, \qquad (1)$$

where $\chi^-_{\mathrm{FORC}}(E_r,E)$ are the differential susceptibilities measured along the FORCs.

The 3D-FORC distribution $\rho(E_r,E)$ describes the sensitivity of polarization in a given sample with respect to changes of the reversal field E_r and actual electric field E. By changing the coordinates of the FORC distribution from (E,E_r) to $\{E_c=(E-E_r)/2,\ E_{\mathrm{bias}}=(E+E_r)/2\}$, where E_c and E_{bias} play the role of local coercive and bias fields, respectively, $\rho(E_c,E_{\mathrm{bias}})$ becomes a distribution of the switchable units over their coercive and interaction (bias) fields.

It is worth stressing that, for CPS, the FORC and Preisach distributions are identical,[32] while, for more complex systems, they might differ significantly (see the discussion about first- and second-order reversal curve diagrams in Ref. 33). When the two distributions are different, the CPM cannot offer adequate explanation; only simulations with more complex models can help in properly understanding their meaning for particular characteristics of the hysteretic systems.[27–29] From the authors' point of view, the main advantage of the FORC method is that it is an experimental, model independent technique which is consequently applicable for describing any ferroic system. Another important advantage of the method is the possibility it offers to evaluate separately the reversible and irreversible contributions to the total polarization by using the same set of experimental data, together with a proper numerical procedure.[32] The reversible part of the FORC distribution, as due to the low-field contributions to the polarization, is calculated as

$$\rho^{\pm}_{\mathrm{rev}}(E_r) = \lim_{E\to E_r, E>E_r} \rho^{\pm}_{\mathrm{FORC}}(E_r,E). \qquad (2)$$

The reversible contribution revealed by FORCs can be compared with the results obtained by other investigations such as the Rayleigh loops or the low-signal capacitance measurements[34] and gives important information on the subswitching regime of the polarization-field dependence in a given ferroelectric system.

In the case of ferroelectrics, it was previously demonstrated that FORC diagrams are sensitive to the frequency of the applied field, crystalline orientation, and fatigue effects.[31] "Healthy" and homogeneous ferroelectrics with rectangular hysteresis loops are characterized by FORC distributions with a sharp maximum located at well defined fields $(E_{cM},E_{\mathrm{bias}M})$ and with almost zero reversible component. Such a sharp distribution was found for high-oriented epitaxial and polycrystalline homogeneous Pb $(Zr,Ti)O_3$ (PZT) films in their fresh state, while broader distributions with an important reversible component are characteristic of the nonhomogeneous and nonoriented ceramics. Particularly, very broad and dispersed FORC distributions were found in ferroelectrics in their fatigued state, due to the local imprint effects.[31] Distributions with multiple maxima were also proposed to describe ferroelectric samples with a certain degree of inhomogeneity, like unpoled ceramics.[12] Thus the FORC distributions are giving fingerprints of the ferroelectric systems on the point of view of their local switching properties.

In parallel with modeling tools aimed to unlock the information contained in these diagrams, it is highly important to find a closer relationship between the FORC diagrams and the microstructures in various systems. So, it is necessary to use this approach in investigating various ferroelectric samples with different switching characteristics derived from their particular microstructures. In the present work, the porous PZT-based ceramics with anisotropic porosity (40% relative porosity) and dense isotropic ceramics (5% relative porosity) having the same composition are comparatively investigated by this method. The porous piezoelectric materials are interesting for application as low frequency hydrophones and sensors, due to their high piezoelectric figure of merit. In past years, a wide variety of methods were developed in order to produce porous structures, such as reticulated polymer foams or volatile additives which are burnt out during the sintering process.[35–37] Anisotropic porosity was recently obtained in Nb-doped PZT ceramics by adding lamellar graphite as a pore forming agent.[38] Peculiar dielectric and piezoelectric properties resulted in such ceramics as a consequence of their distinct microstructures in terms of pore size, morphology, and porosity volume fraction. The influence of closed and open porosity on the macroscopic properties is related to the different electrical and mechanical boundary conditions acting on the ceramic grains in dense/porous materials. The switching properties in such ceramics were not yet systematically investigated. Some peculiar aspects of the switching properties in dense and anisotropic porous Nb-ZT ceramics are investigated by using the FORC analysis. The role of anisotropy in changing the interaction dipolar field is revealed in samples with high anisotropic porosity by comparing the FORC diagrams determined by applying the elec-

trical excitation parallel or perpendicular to the direction of the elongated pores. The obtained results are explained in the frame of a discrete dipolar model by considering the changes of the local field induced by the forward or lateral dipolar coupling. In addition, an algorithm allowing the use of the experimental FORC distribution as input for a Preisach-type model was developed.

II. CERAMIC PREPARATION AND EXPERIMENT

Powders with the nominal composition $Pb(Zr_{0.52}Ti_{0.48})_{0.976}Nb_{0.024}O_3$ were prepared via solid state reaction. The starting oxides with stoichiometric proportion were wet-ball milled with zirconia milling media for 24 h, freeze dried, sieved to 200 μm and calcined at 850 °C for 4 h. Calcined powders were ball milled for 100 h, dried at 90 °C and sieved to 200 μm. In order to obtain porous ceramics, fine grained graphite powders (40% content) were mixed with the calcined Nb-PZT powders. Disk shaped samples with a thickness of 2 mm and a diameter of 25 mm were produced. The sintering was carried out at 1150 °C for 2 h with the samples placed on ZrO_2 disks and covered with Al_2O_3 crucible and sealed with pack ($PbZrO_3$+5 wt. % excess of ZrO_2) in order to avoid the PbO loss during sintering. The structural study by x-ray diffraction did not reveal any important differences between the dense and porous materials in terms of composition and tetragonal distortion. The result is that the major difference in the final microstructures is the degree of porosity only. For the electrical measurements, the ceramics were polished, electroded perpendicularly and respectively parallel to the direction of the applied pressure, and fired at 700 °C. The microstructural characteristics and the dielectric and piezoelectric properties of the samples with homogeneous porosities in the range (0–40%) were previously reported.[38] The graphite develops lamellar porosity preferentially oriented perpendicular to the direction of the applied pressure during the cold pressing step. The samples show tridimensionally interconnected open porosity and the dense part of the porous ceramics has the same microstructural characteristics and density as in the dense sample (small size pores with high mean aspect ratio and randomly aligned, 95% relative density), as presented in Fig. 3. The experimental FORCs and symmetric minor $P(E)$ loops were recorded under a sinusoidal waveform of an amplitude of E_0=2.5 kV/mm and frequency f=1 Hz by using a modified Sawyer-Tower circuit, under a field sequence described before. The results found in a dense (95% relative density) and in a high-porosity sample (60% relative density) are reported for comparison in the present study. In the case of the anisotropic porous sample, the data were collected in both parallel and perpendicular electrode configuration (referring to the direction of the major axis in the elongated pores).

III. RESULTS AND DISCUSSIONS

A. The FORC distributions. The role of porosity

Figure 2 shows a few experimental FORCs obtained for the dense Nb-PZT ceramic. The FORC distributions were

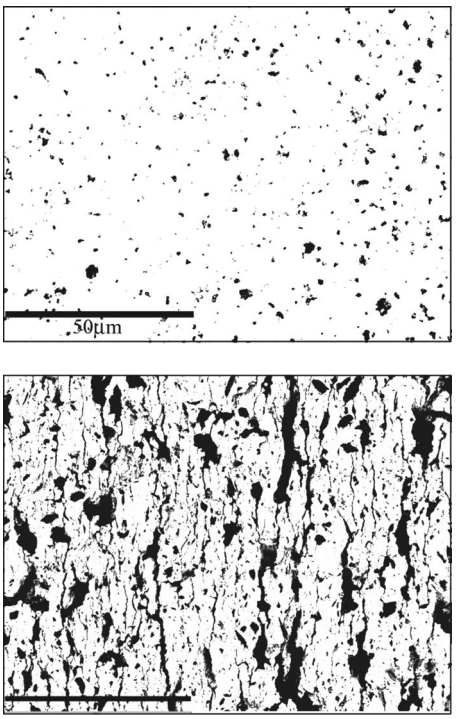

FIG. 3. SEM micrographs of the polished surfaces of the Nb-PZT ceramic. Bar: (a) 50 μm; (b) 500 μm.

calculated from such data following a numerical procedure of interpolation and derivation as described in Ref. 32. The three-dimensional representations of the FORC distributions $\rho(E_r,E)$ obtained for the dense and porous material, respectively, are shown in Figs. 4(a) and 4(b), while the contour plots (i.e., the 2D-FORC diagrams) of the dense and porous ceramic in both configurations are shown in Figs. 5(a)–5(c). Due to the fact that the MHLs recorded before and after performing the FORC experiments were identical, any possible degradation processes (e.g., fatigue) did not alter the state of the ferroelectric system during the experiment itself. Consequently, the experimental FORC distribution of one sample is unique in the limit of experimental and numerical accuracy and describes the switching properties of the ferroelectric system under given conditions.

Both distributions characteristic to the dense and porous ceramics show two well-defined separated components corresponding to the reversible and irreversible contributions to the ferroelectric polarization. The reversible part, caused by domain wall oscillations and lattice intrinsic contributions, is higher in the porous ceramic than in the dense one (Fig. 4): The ratio of the irreversible/reversible maxima of the FORC distributions is around 3/2 for the porous sample and around 11/2 for the dense sample. This big difference in the relative weights of the two contributions to the total polarization shows that in the porous material a large percentage of ferroelectric domains are pinned by local defects and the domain walls can only reverse oscillate under the applied field. Oppositely, for the dense material, the contribution to the total polarization response is mostly determined by the irreversible (switching) domain wall movements.

The irreversible component of the FORC distribution has a well-defined sharp maximum for the dense

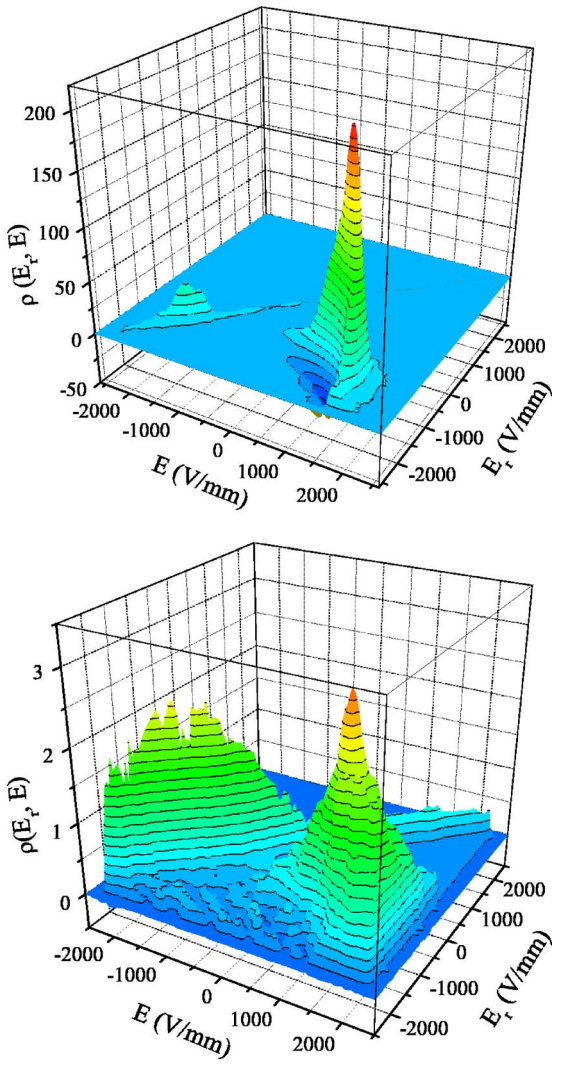

FIG. 4. (Color online) Three-dimensional FORC distributions $\rho_{\mathrm{FORC}}^{-}(E_r,E)$ computed by using the experimental FORCs. The relative weights of the reversible/irreversible parts of the FORC distribution show the contribution to the total polarization of the two types of processes involving domain wall movements under the cycling field.

material [Figs. 4(a) and 5(a)] located at $E_{r,M}=-1.5$ kV/mm and $E_M=1.5$ kV/mm (corresponding to the coercivity $E_{c,M}=1.5$ kV/mm and bias field $E_{\mathrm{bias},M}=0$). These fields represent the most probable values for the reversal and actual field activating the highest number of the system's switchable units, thus causing the highest contribution to the ferroelectric polarization under the specific field sequence. In spite of the fact that the dense ceramic is homogeneous and in its fresh state, the corresponding FORC distribution is far from an ideal Gaussian 3D function over the reversal and actual fields (E_r,E), as proved by Figs. 4(a) and 5(a). This type of distribution was often reported in the nonoriented real ceramics in their unpoled state and was related to the random orientation of the crystallites, to the broad distribution over the ceramic grain size, or to other microstructural effects.[10–12] Therefore, the majority of the switchable units are described by a sharp maximum at the mentioned values

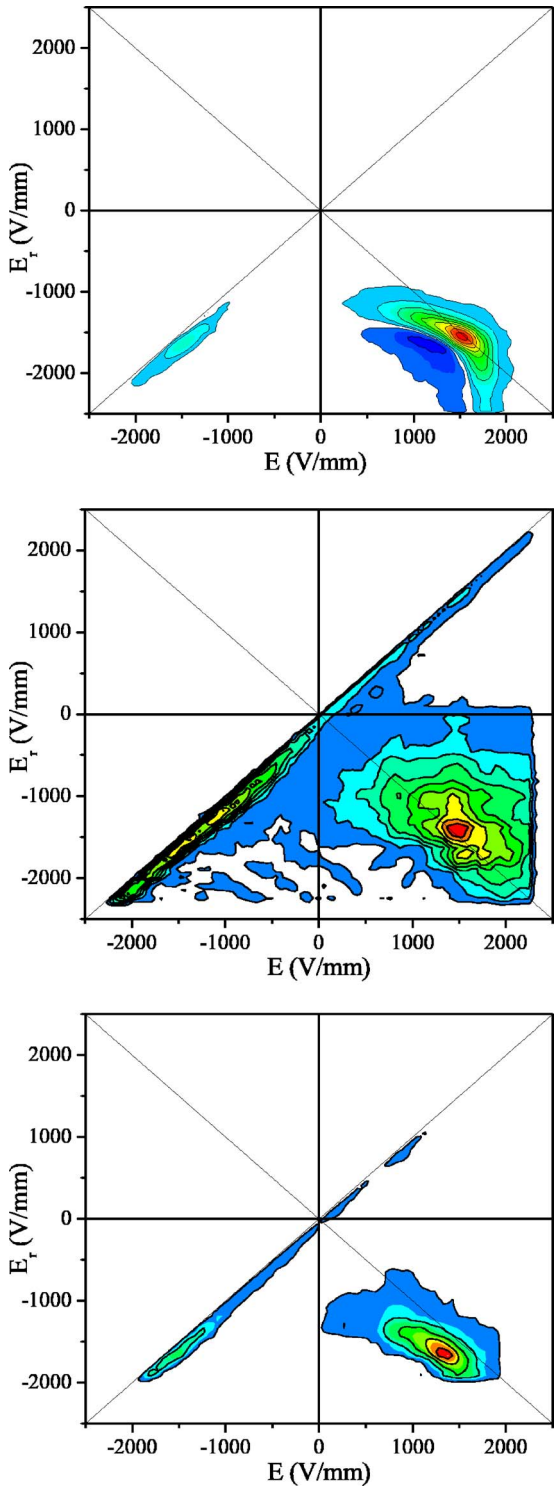

FIG. 5. (Color online) FORC diagram obtained for (a) dense Nb-PZT ceramic, (b) porous Nb-PZT ceramic in parallel configuration (electrodes parallel to the major axis of the elongated pores), and (c) porous Nb-PZT ceramic in perpendicular configuration (electrodes perpendicular to the major axis of the elongated pores).

of fields and the distribution is still characteristic for a homogeneous system. Oppositely, the irreversible component of the FORC distributions obtained for the porous ceramic [Figs. 4(b) and 5(b)] is very broad and dispersed, having a

lower intensity. This means that a large number of dipolar units are spread towards higher/lower values of the reversal and actual fields, due to different local mechanical and electrical boundary conditions. These are causing very scattered local fields acting on individual dipolar units inside the porous material and, consequently, the corresponding FORC diagram is describing a more inhomogeneous ferroelectric system.

The switching characteristics revealed by the observed FORC diagrams can be explained by considering the mechanism of switching in polycrystalline ferroelectrics and the microstructural particularities of the present samples. The polarization reversal (ferroelectric switching) is related to a hysteretic process involving ferroelectric domain dynamics (nucleation, forward, and sideways growth), which has contributions from both reversible and irreversible phenomena. Both components are strongly dependent on the microstructure, particularly on the crystalline symmetry and defect structure. It is generally recognized that the pinning of the domain walls by defects is an important phenomenon particularly at subswitching fields (Rayleigh zone).[39–41] The pinning effect is closely related to charged point defects (dipolar) and interface defects. They also contribute to the complication of the local electric and stress fields within the sample. It is clear that an homogeneous and defect-free ferroelectric sample will show homogeneous switching properties due to the fact that the collective of individual switching units is subjected to very similar local fields and they evolve under the same boundary conditions, thus all giving almost identical contributions to the total polarization. This will give rise to a highly localized and well defined FORC distribution with a sharp maximum of the irreversible component and an almost zero reversible part. The FORC diagram of Fig. 4(a) represents such a diagram characteristic to a "healthy" and homogeneous ferroelectric and correctly describes the switching properties of the dense ceramic in connection with its microstructure.

By comparison, the porous ceramic has rather inhomogeneous switching properties derived from its particular microstructure. First, the ceramic grains are subjected to different boundary conditions if they belong to a dense region or if they are in contact with air pores. Particularly, the presence of air pores relaxes the mechanical clamping. The uncompensated charges located at these interfaces create depolarizing fields, strongly dependent on the pore shape and morphology. Since in the porous ceramics a few types of pore distributions according to their orientations and aspect ratio were identified, a complicated and strongly inhomogeneous picture of the electrical and strain-stress local fields inside the ceramic material results. Moreover, not all the regions equally contribute to the total polarization, also due to the defective structure of the overall sample volume. Some regions might be completely pinned by these defects and thus might not contribute anymore to the irreversible polarization. As mentioned before, uncompensated charges at the ceramic-air interfaces create local depolarizing fields, so that higher fields are necessary to switch the dipolar units than in dense ceramic. In respect to these features, the description of the porous ceramic by a dispersed and broad FORC distribution with a higher contribution of the reversible polarization on the expense of the irreversible one [Figs. 4(b) and 5(b)] is in complete agreement with the expected switching behavior derived from the microstructural characteristics. The characteristic distribution has a broad maximum elongated on the direction $E=E_r$, describing a more distributed range of characteristic coercivities than in the dense material. The elongated maximum is still well defined at almost the same value of coercivity $E_{c,M}=1.5$ kV/mm and has a small positive bias: $E_{\text{bias},M}=50$ V/mm. The observed shifts towards higher values on the fields are in agreement with the microstructural characteristics of the porous material investigated in parallel geometry.

Biased $P(E)$ hysteresis loops are not so common for ceramic materials. Even in our case, the bias field is rather small and is almost impossible to observe by looking to the MHL only. Instead, rather high bias fields were largely reported in many other ferroelectric structures like films[42–46] (recently, in ultrathin structures with thickness down to a few unit cells[45,46]). The value of this bias shift, measuring the total imprint of the polarization, was found as high as the system is thin, i.e., as large as the confinement degree of the system.[47] Its origin is a topic still under debate, in spite of the many hypotheses formulated. Mostly extrinsic contributions, such as electrode and interface effects, low-permittivity polarization-independent and relatively stable layers under the electrodes,[48] pinning of the domain walls by charged defects, strain gradient and lattice distortions between at the ferroelectric/electrode interface,[42–44,49,50] local defects,[47] or space charge phenomena,[51] were considered. Contributions due to the inhomogeneous distribution of the polarization near the surface and depolarization fields associated with incomplete compensation charge at the electrodes probed to occur in very thin (2.5–5 nm) layers in contact with electrodes[52] are important only in ultrathin structures. Since in a bulk ceramic such extrinsic phenomena give a minor contribution, it is proposed that intrinsic phenomena related to the dipolar coupling effects produced by the geometrical confinement are the main source of the built-in bias field in the present porous ceramics. In order to confirm this hypothesis, the role of the microstructural anisotropy on the FORC diagrams is further analyzed.

B. The role of microstructural anisotropy on the FORC diagrams

More complete information about the role of microstructure on the switching properties is obtained by comparing the FORC diagrams obtained for the sample with 40% anisotropic porosity in geometry with electrodes parallel and respectively perpendicular to the direction of the major axis of the elongated pores. Although the composition and degree of porosity is the same, the diagrams found in parallel and perpendicular geometries are clearly different [Figs. 5(b) and 5(c)], due to the anisotropy induced by the elongated shape of the pores only. The FORC diagram in the perpendicular geometry looks more homogeneous and well localized, closer to the shape of distribution found for the dense system [Fig. 5(a)]. The maximum is located around the same coercive field $E_{c,M}=1.5$ kV/mm and shows a small negative bias

$E_{bias,M}=-100$ V/mm (shift of the maximum in the negative direction of the axis E_{bias}). The reversible part is less pronounced than one obtained in the parallel geometry, but is slightly higher than in the dense ceramic. In conclusion, the coercivity is almost the same in all ceramics and for both geometries, while the bias is (a) zero for the dense isotropic ceramic, (b) small and positive for the porous one in parallel configuration, and (c) small and negative for the porous one in perpendicular geometry. The negative/positive values of the bias mean that an average polarizing/depolarizing internal field is acting on the sample. This is related to an asymmetry of the $P(E)$ hysteresis loop on the field axis caused by the preference of a certain polarization state over the other one (imprint), as described by an internal built-in bias field.[42,53] Since the same sample was investigated in both geometries, the possible role of the extrinsic contributions on the bias field is the same in both cases. Thus the geometrical confinement only is producing the different signs of these bias fields found by the FORC analysis in the two configurations.

In order to explain the observed features, the microstructural characteristics of the investigated samples have to be considered. The dense material is isotropic so that each individual dipole is subjected to zero average dipolar interaction field due to the cubic arrangement.[32] The result is that the individual dipoles are mainly subjected to the external field and to negligible internal depolarizing field. Due to this, the irreversible part of the FORC diagram centered on the line $E=E_r$ (on the axis $E_{bias}=0$). In the case of the porous ceramic (40%) measured in parallel configuration, a larger number of dipoles are laterally interconnected than along the field axis. When the dipoles are oriented (under high fields), they give a negative contribution to the total field, i.e., creating a depolarizing field. When the porous ceramic is measured in perpendicular geometry, a larger number of neighbor dipoles along the field axis are interconnected than laterally by the pores and they create a positive dipolar field, i.e., they contribute to the polarizing process. In the FORC representation (Fig. 1), the effect of the bias is observed as a shift of the FORC distribution parallel with the axis $E=E_r$ with a quantity equal to the bias field.[32] It is important to note that for low imprint effects (i.e., almost symmetric experimental MHLs, as in the present case), other methods fail in detecting such a small bias on the polarization-field dependences. Thus the FORC diagrams are useful for probing the depolarizing/polarizing effect possibly caused by various types of asymmetries or anisotropies in a given sample.

One important observation should be made here. There is a difference between the built-in internal field and the depolarizing field (always opposite to the polarization vector) caused by uncompensated charges at interfaces or in spatial regions with polarization gradients.[45,54–59] The influence of the depolarizing field on the ferroelectric, dielectric, and piezoelectric properties, mainly in changing the domain structures and the stability of polarization at small dimensions,[57,59] was largely studied and described within the Landau-Devonshire theory.[54–59] It also contributes to changing the apparent coercivity[59] and is one possible source of the negative bias (depolarizing effect) of the $P(E)$ loops in some ferroelectric structures. Instead, the built-in internal (bias) field, which was probed by the present FORC analysis (and observed in many other structures as already mentioned before), can be either positive or negative, thus having both polarization or depolarization effects. The origin of this bias field can come either from intrinsic or extrinsic causes. In the case of our porous ceramics, it is created by the neighboring dipolar entities whose interaction (coupling) is limited by the specific interfaces and geometry and has an intrinsic origin.

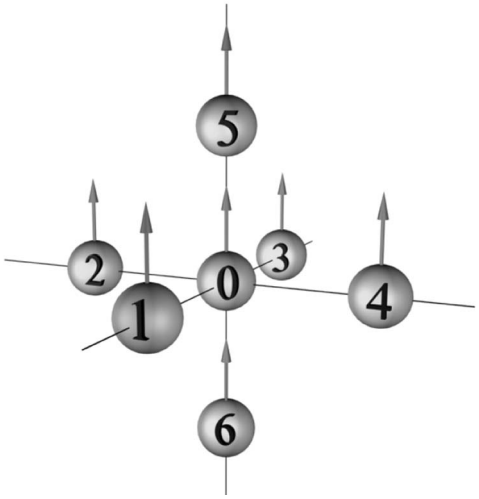

FIG. 6. Representation of the dipolar model system with cubic geometry.

The positive/negative values of the bias fields found in the present porous ceramic as well as the lower values of polarization in parallel geometry are qualitatively explained by considering the dipolar coupling effects. The role of the anisotropic porosity on the bias fields sign was qualitatively demonstrated by computing the FORC diagrams using a discrete dipolar model. The next section presents this approach and the results of these calculations.

C. FORC diagrams calculated with the dipolar model. The effect of the forward/lateral dipolar coupling on the bias fields

The above described role of anisotropy on the FORC diagrams can be explained by using a simple description of the ferroelectric system within a discrete dipolar model. A 3D network of identical interacting dipoles with moments $\vec{p}_i$ in a cubic geometry, as presented in Fig. 6, is first considered. The electric field acting on an individual dipole "i" is the sum of the external field E_{ext} and of the total field $E_{dipoles}$ created by the other dipoles:

$$\vec{E}_i = \vec{E}_{ext} + \vec{E}_{dipoles} = \vec{E}_{ext} + \frac{1}{4\pi\epsilon_0}\sum_{i\neq j}\left(3\frac{\vec{p}_j\cdot\vec{R}_{ij}}{R_{ij}^5} - \frac{\vec{p}_j}{R_{ij}^3}\right), \tag{3}$$

where R_{ij} is the distance between the individual dipoles i and j. By considering just the first-order neighbors' contributions, the field E_0 acting on the central dipole (i.e., the internal field) is zero, due to the cubic symmetry (Fig. 6)

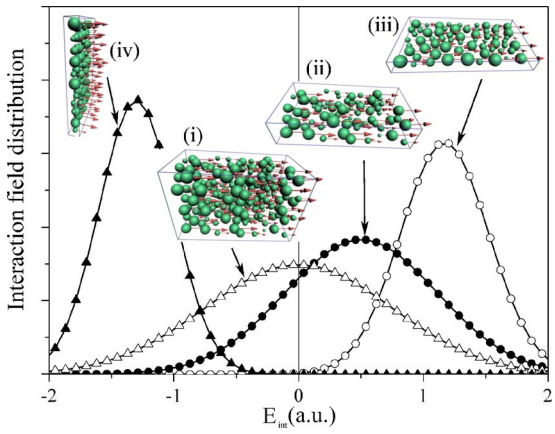

FIG. 7. (Color online) The average distributions of dipoles over the internal fields, calculated for the cubic symmetry and different degrees of lateral confinement (forward or lateral dipolar coupling).

$$\vec{E}_0 = \sum_{i=1,6} \vec{E}_{\text{dipole},i} = \vec{E}_{\text{int}} = 0, \tag{4}$$

since

$$\vec{E}_{\text{dipole},1} + \vec{E}_{\text{dipole},2} + \vec{E}_{\text{dipole},3} + \vec{E}_{\text{dipole},4} = -(\vec{E}_{\text{dipole},5} + \vec{E}_{\text{dipole},6}). \tag{5}$$

For the lateral confinement, the presence of free surfaces created by the anisotropic pores breaks the cubic symmetry and causes a nonzero internal field. This internal field is positive, causing polarizing effect if the dipoles are forward coupled, i.e., the dipole moments are aligned with the long axis of the pore and respectively negative (depolarizing), or laterally coupled, i.e., if the dipole moments are perpendicular to the long axis of the pore. Note that the bias and internal fields are opposite: $E_{\text{bias}}=-E_{\text{int}}$, so that a higher positive than negative field is necessary for switching to compensate the depolarizing effects (negative internal field) and consequently the $P(E)$ loop will be shifted on the field axis towards higher values (positive bias).

In real systems randomness replaces the perfect cubic network. Nevertheless, the presence of the free surfaces has the same effect. For describing this situation a system of a few thousand dipoles randomly distributed in four types of "samples" was employed (Fig. 7): (i) A bulk sample where most of the dipoles are far from any free surface; (ii) a thin sample in-plane polarized where most of the dipoles are forward coupled; (iii) a single layer of dipoles in-plane polarized; and (iv) a single layer of dipoles polarized perpendicular to the plane of the sample, where the dipoles are laterally coupled.

The interaction field acting on a certain dipole was calculated as the vector sum of the fields produced by all of the other dipoles. The statistical distributions of the interaction field for the four cases are represented in Fig. 7.

The computed interaction field distribution at the saturation (i.e., when all the dipoles are oriented along the direction of the external field) is located at $E_{\text{bias}}=0$ for bulk uniform samples and they are shifted over their interaction fields for lateral or forward coupling. The shift of the internal field resulted as positive (i.e., has a polarizing direction, contributing with the internal field to the increasing polarization) if the dipoles are forward coupled and negative (depolarizing effect) if the dipoles are laterally coupled. This shift, measuring shift, measuring the total imprint of the polarization has a higher value for thinner systems, i.e., as large as the ratio of the dipoles very close to a free surface. The results for the simulated "samples" are presented in Fig. 7, parts (i), (ii), and (iii).

Using the mean interaction field, the calculated FORC distributions show the following types of built-in internal fields: (a) $E_{\text{int}}=0$—corresponding to geometry (i) in Fig. 7, (b) $E_{\text{int}}<0$—corresponding to geometry (ii) in Fig. 7, and (c) $E_{\text{int}}>0$—corresponding to geometry (iv) in Fig. 7, which are represented in Figs. 8(a)–8(c), respectively.[32] The confinement results in a change of the position of the maximum corresponding to the irreversible FORC component in a positive or negative direction.

The same trend was observed in the experimental FORCs determined for the dense ceramics and the porous one in the two configurations (Fig. 5). This calculation demonstrated that the built-in bias field can also have an intrinsic origin related to the dipolar nature of the system and its particular geometry leading to a specific character of the dipolar coupling and not only extrinsic ones, as generally proposed for ferroelectric confined structures.[42–46,54–59] In the particular case of the bulk ferroelectric ceramic with anisotropic porosity, the different signs of the bias fields found in the two configurations have a fully intrinsic nature resulting from the geometric confinement effect.

The physics of the switching process in ferroelectric ceramics is rather complicated, particularly for inhomogeneous and defective systems, due to many local parameters and boundary conditions determining the ferroelectric properties. In addition, various contributions to the polarization response under driven fields are expected, besides the dipolar ones. Here a very simplified dipolar model was first employed. Due to the simplicity of this approach, in which no reversible contributions were considered, we cannot expect to find a full correspondence between the simulated and experimental FORC diagrams of Figs. 5 and 8. In fact, in Fig. 8 only the irreversible distributions were obtained. In order to better describe the anisotropic porous ceramic response, further development of the dipolar approach is necessary. For quantifying the confinement effects associated with the porosity, various "samples" containing both lateral and forward dipolar coupling with various weights (series-parallel interconnected) and with geometrical parameters related to the pore size distribution and orientation have to be "built" for simulations. In addition, the experimental response of various ceramics with the same compositions and different degrees of porosity and shape anisotropy have to be obtained for comparison. Such a complex investigation was beyond our present work. Even very simplified, the employed dipolar model in which the contribution of the first-order neighbors was considered is able to describe qualitatively the positive/negative bias fields obtained in the FORC diagrams of the anisotropic porous PZT and zero bias in the dense isotropic material, while the coercive field corresponding to the maximum is always the same.

D. Simulation of switching properties using the FORC distribution and comparison with the experimental data

The attempts used in literature for modeling the ferroelectric hysteretic behavior are either based on simplified empirical expressions [as for example combinations of hyperbolic $P(E)$ functions],[60] or on Landau-type models with adjustable parameters considering the microstructural and degradation effects.[61,62] Other categories of theoretical approaches are rather complicated, with a large number of parameters and iteration procedures of identification for considering the local mechanical and electrical history in building macroscopic models.[63] The majority are unable to satisfactorily and completely describe the hysteretic behavior under arbitrary applied fields. A simplified version of the Preisach approach using analytic functions[7,8] or more complex ones, based on the superposition of some Preisach functions,[64,65] were also employed. In spite for their incontestable usefulness for giving descriptions of the switching-related properties in ferroelectrics, the majority are unable to simulate the polarization-field $P(E)$ response under arbitrary applied fields and very poor agreement of the calculated $P(E)$ dependencies is obtained, particularly for nonsaturated loops or in systems with a certain degree of inhomogeneity or ferroelectric degradation.

By considering that in the limit of experimental and numerical accuracy the experimental FORC distribution is fully describing the present hysteretic system, the polarization under any field sequence and history can now be calculated. This possibility can be further used to simulate the responses of circuits containing ferroelectric capacitors in various applications and is particularly useful for designing and describing integrated ferroelectric memory devices. For example, the MHL and symmetric minors of the Nb-PZT dense ceramic with various amplitudes were simulated, by numerical integration of the determined FORC distribution under specific field history.

In general, the experimental FORC distributions are asymmetrical with respect to the second diagonal of the coordinate system (the coercive field axis—Fig. 1). One of the causes for this asymmetry, already described before, is the state dependence of the width and position of the interaction field distribution's maximum. In fact, the FORC diagram is far from the conventional projection of a static Preisach-type distribution, but rather is a static representation of a dynamic distribution.[66] Thus the simple numerical integration of the FORC diagram using the CPM algorithm would lead to unsatisfactory results—even for the descending branch of the major hysteresis loop. Moreover, it would lead to asymmetrical MHLs (i.e., loops for which the lower and the upper branches are not symmetrical with respect to the origin of the coordinate system). An important remark is that if one computes the FORC diagram using the descending reversal curves (not the ascending ones as in Fig. 2), a diagram which is the mirrored version of the first FORC diagram with the respect of the second diagonal of the coordinate system is obtained. For a more realistic approach, it is proposed here to use both FORCs $p^{\pm}_{\mathrm{FORC}}(E_r,E)$ (where "+" stands for the measurement starting from the reversal points found on the descending major hysteresis branch and "−" for the measurement starting from the reversal points found on the ascending major hysteresis branch) in an algorithm similar to the one previously designed for the PM2 model.[66] This approach is proven to include both a mean interaction field and

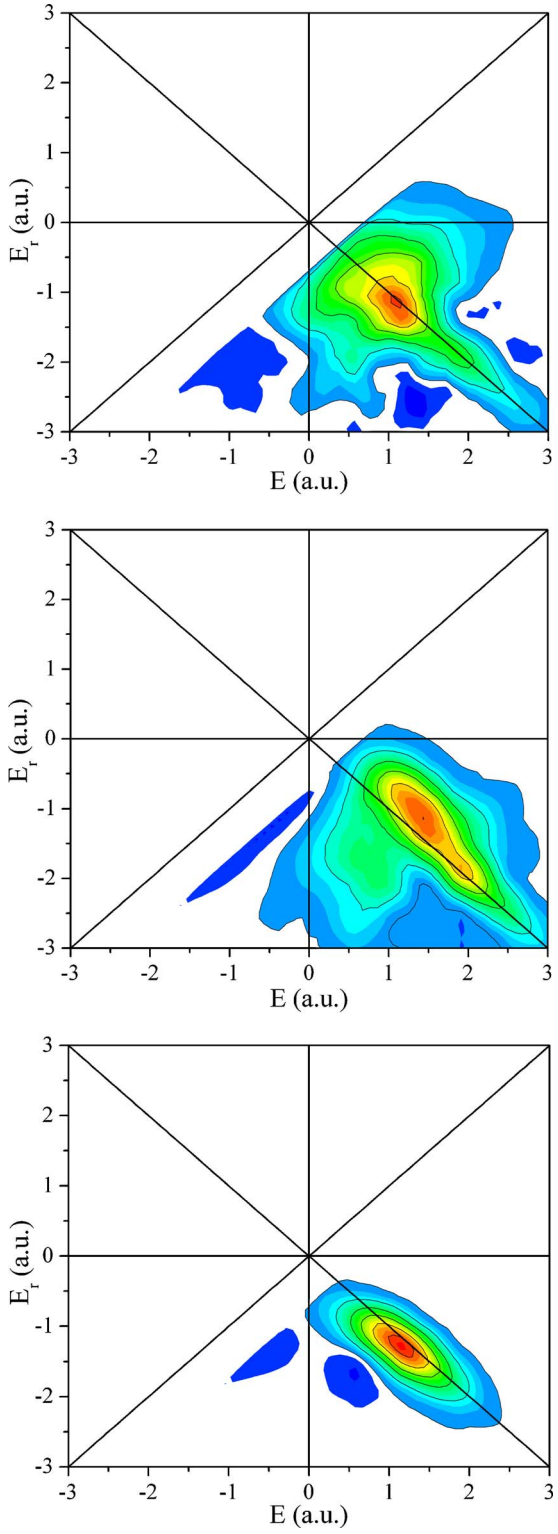

FIG. 8. (Color online) Computed FORC diagrams within the dipolar model by considering (a) $E_{\mathrm{int}}=0$, (b) $E_{\mathrm{int}}<0$, and (c) $E_{\mathrm{int}}>0$ corresponding to the "samples" (i), (ii), and (iv) from Fig. 7, respectively.

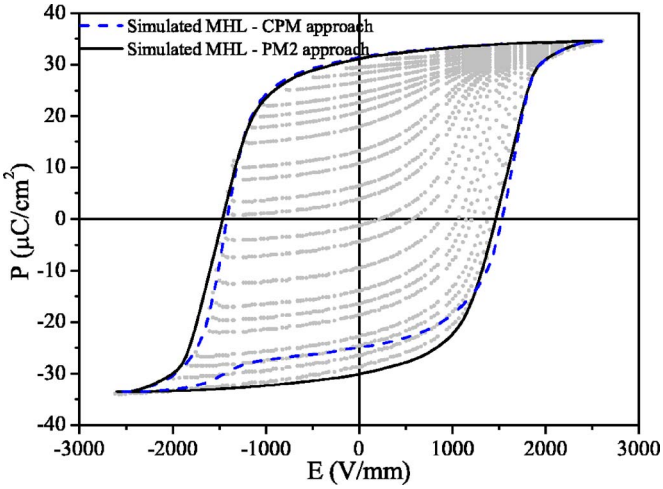

FIG. 9. (Color online) Numerical reconstruction of the MHL of the dense Nb-PZT ceramic by using the Preisach approach with CPM and PM2 approaches.

variable variance effects. In the proposed algorithm,[66] the state-dependent distribution is given by

$$p_{\mathrm{FORC}}(E_r,E) = \frac{(1+E)}{2}p^{+}(E_r,E) + \frac{(1-E)}{2}p^{-}(E_r,E) \quad (6)$$

and then is integrated as in CPM in order to calculate the response of the system:

$$P(E_r,E) = \int\int_{E_r,E} p_{\mathrm{FORC}}(E_r,E)dE_r dE. \quad (7)$$

The results for the reconstruction of the MHL curve using the experimental FORC distribution in Fig. 5(a) are represented in Fig. 9. They show very good agreement with the original MHL data, particularly one that resulted as applying the PM2 model, for which the coefficient of determination[67] between the computed polarizations and the experimental values is $R^2=0.9956$. Also the computed minor symmetric loops from Fig. 10(a) are very similar to the experimental ones presented in Fig. 10(b).

Once determined, the FORC distribution can be used to simulate different polarization experiments and nonlinear responses of circuits containing ferroelectric capacitors within circuit simulators such as SPICE or others.[68–70] It is known that circuit simulation is essential in designing large scale and high-speed devices and ensuring their reliability. However, there is high difficulty in calculating the response when ferroelectric capacitors are employed, because of their complicated behavior which cannot be described properly by simple models. In this spirit, the FORC distribution is easily accessible and gives a more complete description of the polarization response than any type of analytic function. Even though the FORC diagram might be dependent on the experimental conditions and field characteristics, those simulated responses are useful for giving reference values for the outputs involving the ferroelectric polarization under various experimental conditions.

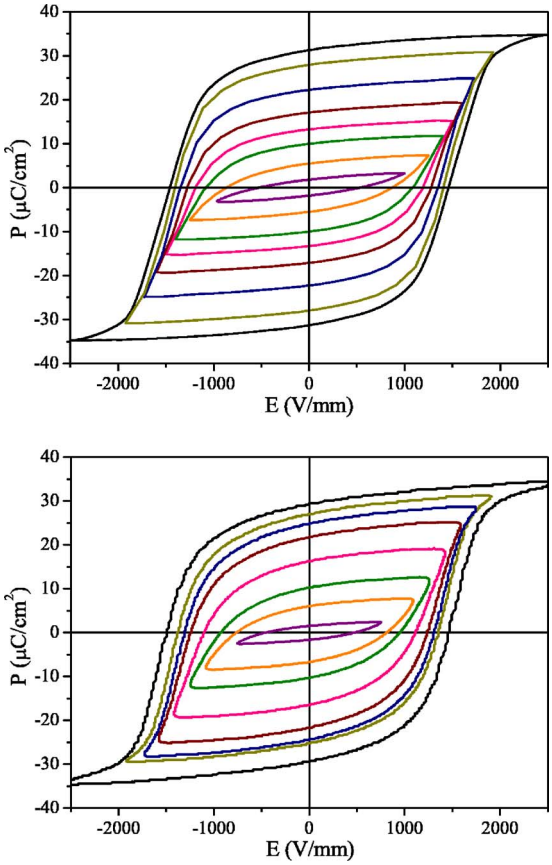

FIG. 10. (Color online) Symmetric minor loops of the dense Nb-PZT ceramic at a few values of the field amplitudes: (a) Computed from the experimental FORC distribution within the PM2 approach; (b) determined experimentally.

In conclusion, the FORC approach is a relatively easy method of characterization of the ferroelectrics that might become a valuable standard way of describing the sample properties allowing one to obtain information about the the complex ferroelectrics physics at the local level. However, more effort is needed for a proper interpretation of the FORC diagrams, i.e., for unlocking the rich information contained in it. In this spirit, there is a further need to (i) apply the method on a large number of various ferroelectric systems characterized by different microstructures and intrinsic properties and (ii) to perform simulations of polarization experiments within simple models, to compute the theoretical FORC diagrams, and to examine their sensitivity to various model parameters.

IV. CONCLUSIONS

A first-order reversal curve (FORC) analysis was performed in order to describe the switching properties of Nb-PZT ceramics with anisotropic porosity (40% relative porosity) by comparison with the dense and isotropic one (5% relative porosity). The experimental FORC diagrams have two distinct parts attributed to the reversible and irreversible components of the ferroelectric polarization. A more localized distribution with almost negligible reversible com-

ponent was found in the dense material, while in the porous one the FORC distribution is broader and has a larger reversible component. The irreversible part of the FORC distribution has a well-defined sharp maximum for the dense material located at the coercivity and internal fields of $E_{c,M}=1.5$ kV/mm and $E_{\text{bias},M}=0$, respectively. These fields represent the most probable values for the reversal and actual fields activating the highest number of the switchable units of the system, thus causing the highest contribution to the ferroelectric polarization under the specific field sequence. The coercivity corresponding to the maximum is the same in the porous sample, both in parallel and perpendicular configuration, while the bias fields are (a) small and positive $E_{\text{bias},M}=50$ V/mm in parallel geometry and (b) negative $E_{\text{bias},M}=-100$ V/mm in perpendicular geometry. The influence of the dipolar coupling giving such types of bias fields in the two cases was explained taking into account the long range character of the ferroelectric order. Thus, in particular microstructures with elongated pores, the cubic symmetry is broken, causing the forward or laterally decoupling of the dipolar interaction. A dipolar model with random orientations of the dipoles' directions was used to simulate this confinement effect. The calculated FORC diagrams lead to the same type of bias as the experimental ones. This approach qualitatively demonstrated that the lateral confinement is an intrinsic contribution to the biased $P(E)$ loops for the porous ceramics and, more generally, is one of the possible mechanisms used to create the built-in field in confined ferroelectric structures. The FORC distribution determined by experimental data was also used to recompose the major (MHL) and the minor symmetric hysteresis loops $P(E)$ that resulted in very good agreement with the experimental ones. With precautions related to the fact that the FORCs can be dependent on the experimental conditions and field characteristics in a given experiment and within the limit of accuracy due to experimental and numerical errors in determining the FORC diagrams, the method is a useful tool for describing the ferroelectric systems, to simulate various polarization experiments, and to predict outputs of the circuits containing ferroelectric capacitors. In addition, the FORC approach is sensitive to microstructural parameters and gives a description of some switching characteristics of a ferroelectric sample. Given the relative ease of obtaining experimental data required for calculating the FORC diagrams using modern ferroelectric testing equipment, it may not be long until this method becomes a standard characterization for ferroelectric capacitors and memories, as is already used for ferromagnetic materials.

ACKNOWLEDGMENTS

The financial support of the COST 525 Action (STMs at ISTEC-CNR Faenza, Italy of L.M. and L.S.) is highly acknowledged. The work was also supported by the SPINNER project, Region Emilia Romagna, Italy and by the CEEX for Young Researchers and AC (Consortium) grants of the Romanian CNCSIS.

[1] F. Preisach, Z. Phys. **94**, 277 (1935).
[2] I. D. Mayergoyz, J. Appl. Phys. **57**, 3803 (1985).
[3] I. D. Mayergoyz, Phys. Rev. Lett. **56**, 1518 (1986).
[4] I. D. Mayergoyz and T. A. Keim, J. Appl. Phys. **67**, 5466 (1990).
[5] R. Rammel and J. Souletie, in *Magnetism of Metals and Alloys*, edited by M. Cryot (North-Holland, Amsterdam, 1980).
[6] A. V. Turik, Sov. Phys. Solid State **5**, 1751 (1964).
[7] A. T. Bartic, D. J. Wouters, H. E. Maes, J. T. Rickes, and R. M. Waser, J. Appl. Phys. **89**, 3420 (2001).
[8] G. Robert, D. Damjanovic, N. Setter, and A. V. Turik, J. Appl. Phys. **89**, 5067 (2001).
[9] V. Meyer, J. M. Sallese, and P. Fazan, Ferroelectrics **268**, 251 (2002).
[10] L. Cima and E. Labouré, Rev. Sci. Instrum. **73**, 3546 (2002).
[11] L. Cima and E. Labouré, Ferroelectrics **288**, 11 (2003).
[12] L. Cima and E. Labouré, J. Appl. Phys. **95**, 2654 (2004).
[13] C. H. Tsang and F. G. Shin, J. Appl. Phys. **93**, 2861 (2003).
[14] R. Tanasa, C. Enachescu, A. Stancu, J. Linares, E. Codjovi, F. Varret, and J. Haasnoot, Phys. Rev. B **71**, 014431 (2005).
[15] C. Enachescu, R. Tanasa, A. Stancu, F. Varret, J. Linares, and E. Codjovi, Phys. Rev. B **72**, 054413 (2005).
[16] I. D. Mayergoyz, *Mathematical Models of Hysteresis* (Springer-Verlag, New York, 1991).
[17] G. Bertotti, V. Basso, and G. Durin, J. Appl. Phys. **79**, 5764 (1996).
[18] A. Gruverman, O. Auciello, J. Hatano, and H. Tokumoto, Ferroelectrics **184**, 11 (1996).
[19] L. Eng, M. Friedrich, J. Fousek, and P. Gunter, Ferroelectrics **186**, 49 (1996).
[20] M. Abplanalp and P. Gunter, *Proceedings of the 11th IEEE International Symposium on Appl. of Ferroel. ISAF'98* (Montreaux, Switzerland, 1998), p. 423.
[21] C. Harnagea, Ph. D. thesis, Martin Luther-Universitat Halle, Germany, 2001.
[22] C. Harnagea, A. Pignolet, M. Alexe, and D. Hesse, Integr. Ferroelectr. **44**, 113 (2001).
[23] J. A. Christman, S. H. Kim, H. Maiwa, J. P. Maria, B. J. Rodriguez, A. I. Kingon, and R. J. Nemanich, J. Appl. Phys. **87**, 8031 (2000).
[24] D. Ricinschi and M. Okuyama, Appl. Phys. Lett. **81**, 4040 (2002).
[25] S. V. Kalinin, A. Gruverman, and D. A. Bonnell, Appl. Phys. Lett. **85**, 795 (2004).
[26] E. M. Lines and A. M. Glass, *Principles and Applications of Ferroelectric and Related Materials* (Oxford, New York, 1977), p. 109.
[27] C. R. Pike, A. P. Roberts, and K. L. Verosub, J. Appl. Phys. **85**, 6660 (1999).
[28] C. R. Pike, A. P. Roberts, and K. L. Verosub, Geophys. J. Int. **145**, 721 (2001).
[29] H. G. Katzgraber, F. Pazmandi, C. R. Pike, K. Liu, R. T. Scalettar, K. L. Verosub, and G. T. Zimanyi, Phys. Rev. Lett. **89**, 257202

(2002).
[30] C. Enachescu, R. Tanasa, A. Stancu, E. Codjovi, J. Linares, and F. Varret, Physica B **343**, 15 (2004).
[31] D. Ricinschi, L. Mitoseriu, A. Stancu, P. Postolache, and M. Okuyama, Integr. Ferroelectr. **67**, 103 (2004).
[32] A. Stancu, C. R. Pike, L. Stoleriu, P. Postolache, and D. Cimpoesu, J. Appl. Phys. **93**, 6620 (2003).
[33] A. Stancu, L. Stoleriu, and P. Andrei, J. Appl. Phys. **99**, 08D702(2006).
[34] D. Bolten, U. Boettger, and R. Waser, J. Appl. Phys. **93**, 1735 (2003).
[35] C. R. Bowen, A. Perry, A. C. F. Lewis, and H. Kara, J. Eur. Ceram. Soc. **24**, 541 (2004).
[36] Z. He, J. Ma, and R. Zhang, Ceram. Int. **30**, 1353 (2004).
[37] E. Roncari, C. Galassi, F. Craciun, C. Capiani, and A. Piancastelli, J. Eur. Ceram. Soc. **21**, 409 (2001).
[38] C. Galassi, D. Piazza, and C. Capiani, J. Eur. Ceram. Soc. **25**, 3075 (2005).
[39] D. A. Hall, J. Mater. Sci. **36**, 4575 (2001).
[40] D. V. Taylor and D. Damjanovic, J. Appl. Phys. **82**, 1973 (1997).
[41] D. V. Taylor and D. Damjanovic, Appl. Phys. Lett. **73**, 2045 (1998).
[42] W. L. Warren, H. N. Al-Shareef, D. Dimos, B. A. Tuttle, and G. E. Pike, Appl. Phys. Lett. **68**, 1681 (1996).
[43] M. Alexe, C. Harnagea, D. Hesse, and U. Goesele, Appl. Phys. Lett. **79**, 242 (2001).
[44] T. Tamura, Y. Arimoto, and H. Ishiwara, Jpn. J. Appl. Phys., Part 1 **41**, 2654 (2002).
[45] D. D. Fong, G. B. Stephenson, S. K. Streiffer, J. A. Eastman, O. Auciello, P. H. Fuoss, and C. Thompson, Science **304**, 1650 (2004).
[46] C. Lichtensteiger, J. M. Triscone, J. Junquera, and P. Ghosez, Phys. Rev. Lett. **94**, 047603 (2005).
[47] Y. S. Kim, D. H. Kim, J. D. Kim, T. W. Noh, J. H. Kong, Y. D. Park, S. D. Bu, and J. G. Yoon, J. Korean Phys. Soc. **46**, 55 (2005).
[48] M. Grossmann, O. Lohse, D. Bolten, U. Boettger, T. Schneller, and R. Waser, J. Appl. Phys. **92**, 2680 (2002).
[49] A. Gruverman, B. J. Rodriguez, A. I. Kingon, R. J. Nemanich, A. K. Tagantsev, J. S. Cross, and M. Tsukada, Appl. Phys. Lett. **83**, 728 (2003).
[50] M. Paturzo, P. Ferraro, S. Grilli, D. Alfieri, P. de Natale, M. de Angelis, A. Finizio, S. de Nicola, G. Pierattini, F. Caccavale, D. Callejo, and A. Morbiato,Opt. Express **13**, 5416 (2005).
[51] D. Fu, K. Suzuki, K. Kato, and H. Suzuki, Appl. Phys. A: Mater. Sci. Process. **80**, 1067 (2005).
[52] A. G. Zembilgotov, N. A. Pertsev, H. Kohlstedt, and R. Waser, J. Appl. Phys. **91**, 2247 (2002).
[53] J. Lee and R. Ramesch, Appl. Phys. Lett. **68**, 484 (1996).
[54] M. E. Drougard and R. Landauer, J. Appl. Phys. **30**, 1663 (1959).
[55] S. Triebwasser, Phys. Rev. **118**, 100 (1960).
[56] I. P. Batra, P. Wurfel, and B. D. Silverman, J. Vac. Sci. Technol. **10**, 687 (1973).
[57] M. D. Glinchuck, E. A. Eliseev, V. A. Stephanovich, and R. Farhi, J. Appl. Phys. **93**, 1150 (2003).
[58] V. Nagarajan, S. Prasertchoung, T. Zhao, H. Zheng, J. Ouyang, R. Ramesh, W. Tian, X. Q. Pan, D. M. Kim, C. B. Eom, H. Kohlstedt, and R. Waser,Appl. Phys. Lett. **84**, 5225 (2004).
[59] M. Dawber, P. Chandra, P. B. Littlewood, and J. F. Scott, J. Phys.: Condens. Matter **15**, L393 (2003).
[60] S. L. Miller, J. R. Schwank, R. D. Nasby, and M. S. Rodgers, J. Appl. Phys. **70**, 2849 (1991).
[61] D. Ricinschi, C. Harnagea, C. Papusoi, L. Mitoseriu, V. Tura, and M. Okuyama, J. Phys.: Condens. Matter **10**, 477 (1998).
[62] D. Ricinschi and M. Okuyama, Appl. Phys. Lett. **81**, 4040 (2002).
[63] R. C. Smith, A. G. Hatch, B. Mukherjee, and S. Liu, J. Intell. Mater. Syst. Struct. **16**, 713 (2005).
[64] C. H. Tsang, C. K. Wong, and F. G. Shin, J. Appl. Phys. **98**, 074101 (2005a).
[65] C. H. Tsang, C. K. Wong, and F. G. Shin, J. Appl. Phys. **98**, 084103 (2005b).
[66] A. Stancu, L. Stoleriu, P. Postolache, and R. Tanasa, J. Magn. Magn. Mater. **290-291**, 490 (2005).
[67] I. Stegun and M. Abramowitz, *Handbook of Mathematical Functions with Formulas, Graphs, and Mathematical Tables* (Dover, New York, 1965).
[68] A. Sheikholeslami, P. G. Gulak, H. Takauchi, H. Tamura, H. Yoshioka, and T. Tamura, IEEE Trans. Ultrason. Ferroelectr. Freq. Control **47**, 784 (2000).
[69] K. Dragosits and S. Selberherr, IEEE Trans. Electron Devices **48**, 316 (2001).
[70] H. T. Lue and C. J. Wu, IEEE Trans. Ultrason. Ferroelectr. Freq. Control **50**, 5 (2003).